INSTITUTE OF PLASMA PHYSICS

NAGOYA UNIVERSITY

Single-Electron Capture into Ar^+ Excited States in Ar^{2} + Na Collision below 12 keV.

II. Relative Population Distribution in Ar^+ Excited States.

Atsushi MATSUMOTO,† Seiji TSURUBUCHI,†
Kazuhiko OKUNO,†† Shunsuke OHTANI,
Tsuruji IWAI and Yozaburo KANEKO

IPPJ- 411 Aug. 1979

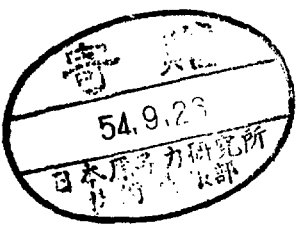

RESEARCH REPORT

NAGOYA, JAPAN

Single-Electron Capture into Ar^+ Excited States in Ar^{2} + Na Collision below 12 keV.

II. Relative Population Distribution in Ar^+ Excited States.

Atsushi MATSUMOTO,† Seiji TSURUBUCHI,†
Kazuhiko OKUNO,†† Shunsuke OHTANI,
Tsuruji IWAI and Yozaburo KANEKO

IPPJ- 411 Aug. 1979

(Received July 24 1979)

Further communication about this report is to be sent to the Research Information Center, Institute of Plasma Physics, Nagoya University, Nagoya, Japan.

---

† Permanent address: Department of Physics, Faculty of Science, Osaka University, Toyonaka, Osaka 560.

†† Permanent address: Department of Physics, Faculty of Science, Tokyo Metropolitan University, Setagaya-ku, Tokyo 158.

Abstract

Excitation cross-sections are obtained for each term of the ArII nl-states (nl=4p, 4p' and 4d) at 4 and 8 keV. The relative population distribution among the terms of a given nl-state can be interpreted in terms of statistics based on the building-up principle of molecule under radial coupling scheme. The relative population distribution among the multiplets in a given term is proportional to their statistical weight; spin-orbit recoupling at large internuclear separations is responsible for the population mechanism. The energy dependence of excitation cross-sections is discussed in connection with the Landau-Zener theory.

§1. Introduction

In our preceding paper (referred to as I), we have reported the spectroscopic study of radiative charge transfer in the collision of Ar^{2+} with Na.[1] According to I, a dominant inelastic collision process is single-electron capture into the excited state of projectile,

$$Ar^{2+} + Na \rightarrow Ar^{+*} + Na^{+} + \Delta E, \qquad (1.1)$$

provided that the energy defect ΔE is a few eV at several-keV collisions. Such an electron capture process is in general described by the potential curves of quasimolecule formed by the collisional pair. At the first approximation, the initial-state interaction can be expressed by a polarization potential between the reactant pair Ar^{2+} + Na, while the final-state interaction is dominated by the Coulomb repulsion between the product pair Ar^{+*} + Na^{+}. If the reaction is exothermic ($\Delta E>0$), the potential curves having the same symmetry pseudocross at some internuclear separation R_c. The well-known Landau-Zener formula for the transition probability in the pseudocrossing region gives rough but very useful estimates of the cross-sections for electron capture.[2] If $\Delta E<0$ (endothermic), there is no crossing in the potential curves. Demkov has given a semiquantitative description of the capture process[3] based on an extension of the Rosen-Zener model.

An accurate theoretical treatment of the electron capture process is time consuming and sometimes practically impossible for

the multielectron system. In spite of their limitations,[3-5] the above-mentioned theories give probably the most useful procedure for estimation of the cross-section at present. Recently, Olson, Smith and Bauer have given a semiempirical formula to estimate the coupling matrix element H_{12} between the reactant and product systems from readily available atomic data such as ionization potential and atomic energy level.[6] Subsituting those values of H_{12} and R_c into the Landau-Zener formula, we can easily evaluate the cross-section for single-electron capture into excited states for exothermic reactions. Olson has extended his semiempirical procedure to a Demkov-type transition and has made it possible to estimate the electron-capture cross-section for endothermic reactions.[7]

These theories, however, are based on the two-state approximation in essence. The present collision system is very complicated by a number of potential curves arising from the collisional pair. Such a complexity is inevitable, as far as the collision of the multielectron system is concerned. Therefore, it will be important to search some guiding rule for giving a perspective view on the electron capture process accompanied with many channels. We shall deal with this problem on the basis of the building-up principle of molecule and statistical considerations in §2. The energy dependence of the excitation cross-section will be discussed in connection with the Landau-Zener theory in §3; concluding remarks follow in §4.

§2. Statistical Consideration on Relative Population Distribution

2a) Experimental result and general description

As mentioned in I, the excitation cross-section for the electron capture into the j-th term of the ArII nl-state† $Q_j(nl)$ follows from the emission cross-section observed (see eqs. (3.3) and (3.4) in I). The values of $Q_j(nl)$ obtained at 4 and 8 keV are listed in Table 1 for the ArII 4p-, 4p'- and 4d-states. Comparison of $Q_j(nl)$ among the product terms of the nl-state gives the relative population distribution among these terms; the column a. of Table 1 represents this distribution. There is some difference between the two distributions at 4 and 8 keV. However, a largely-populated term at 4 keV is still populated largely at 8 keV; a slightly-populated term at 4 keV slightly at 8 keV. Such a trend will be understood by statistical consideration described below.

Figure 1 shows the approximate diabatic potential curves arising from the reactant pair, $Ar^{2+}(3p^4\ {}^3P \text{ or } {}^1D) + Na(3s)$, and from the product pair, $Ar^+(3p^4nl) + Na^+(2p^6)$; the polarization interaction is ignored for simplicity. The potential curve from the product pair observed is represented by a hatchmarked band. The band should contain possible molecular states arising from the possible terms of the ArII nl-state paired with Na^+. Similarly, the potential curve from the reactant pair should contain the corresponding molecular states. As Lichten pointed out,[8] a mixing among the molecular states closely-spaced happens during the collision and

---

†As in I, nl and nl' are the abbreviation of $(3p^4[{}^3P]nl)$ and $(3p^4[{}^1D]nl')$, respectively.

a good measure of the mixing is given by the uncertainty principle; $\Delta U \Delta t \sim 1$, where ΔU is uncertainty in energy of a given state and Δt the collision time. For the present experiment, a typical interaction region is $\sim$10 a.u., a typical velocity $\sim$0.1 a.u. (at 8 keV) and, therefore, a typical collision time $\sim$100 a.u.; ΔU is then $\sim$0.3 eV. This uncertainty in energy is comparable with the width of the hatchmarked band. Consequently, molecular states lying in a band will be well mixed at several-keV collisions. As a result, it seems as if the mixed states were degenerate; the relative population among these states will be governed mainly by statistics[††]. This is our starting point to deal with the relative population among the product terms of the ArII nl-state.

---

††Separations between the bands are a few eV, so that an effective mixing will not be expected between them at several-keV collisions. Thus, for example, the formation process of the ArII 4d-state will be in competition with the one of the ArII 4p-state.

2b) Relative population distribution for ArII 4p-state

To begin with, we consider the process of the electron capture into the ArII 4p-state; $Ar^{2+} + Na(3s,^2S) \rightarrow Ar^+(3p^4[^3P]4p) + Na^+(2p^6,^1S)$. When Ar^{2+} and Na approach each other, a quasimolecule $(Ar, Na)^{2+}$ is formed and diabatic transitions will take place between the quasimolecular states. If the primary ion is assumed to be in its ground state $Ar^{2+}(3p^4,^3P)$, possible molecular terms arising from the reactant pair are obtained from the Wigner=

Witmer rule[9] as follows: $^4\Pi$, $^4\Sigma^-$, $^2\Pi$, and $^2\Sigma^-$. In a similar way, possible molecular terms are obtained from the product pair. There are two dominant coupling schemes for the diabatic transition; one is radial coupling and the other is rotational coupling.[10] Radial coupling must be predominant for the present case, because pseudocrossings appear at large internuclear separations ($R_c \approx 10$ a.u.) and because of low-velocity collisions ($\approx 10^7$cm/sec). Then, transition can take place between the molecular states of the same symmetry and of the same spin; the $^4\Pi$ term from the reactant pair correlates to the $^4\Pi$ terms from the product pair, the $^4\Sigma^-$ term to the $^4\Sigma^-$ terms, and so on. Such a correlation diagram is illustrated in Fig. 2.

The $Ar^{2+}(3p^4, {}^3P)$ term consists of three multiplets $^3P_0$, $^3P_1$ and $^3P_2$, each of which is one-, three- and five-fold degenerate, while $Na(3s, {}^2S)$ is two-fold degenerate. Therefore, the state of the reactant pair is considered to be composed of eighteen sublevels in total. This number of sublevels is conserved in the molecular state and is distributed among the molecular terms; the $^4\Pi$ term has eight sublevels, $^4\Sigma^-$ four sublevels, $^2\Pi$ four sublevels and $^2\Sigma^-$ two sublevels, as denoted by the figure in parentheses in Fig. 2. First we assume that donor channels having the same number as that of sublevels are opened to the molecular state arising from the product pair , and that the donor channels are divided equally between the transition-allowed molecular terms, as shown by arrows in Fig. 2. Next we assume that the number of channels accepted with individual product terms is proportional to the relative population among the product terms; the number of accepted channels is shown by the figure in square brackets in Fig. 2. This is a

present idea based on the building-up principle of the molecule and statistical considerations. The relative population estimated in this way is presented in the column b. of Table 1 and is compared with the one obtained from excitation cross-sections in Fig. 3. Agreement between them is fairly good.

2c) Relative population distribution for ArII 4p'- and 4d-states

Let us apply the statistics just mentioned to the process of electron capture into the ArII 4p'-state; $Ar^{2+} + Na \rightarrow Ar^{+}(3p^{4}[^{1}D]4p') + Na^{+}(^{1}S)$. The 4p'-state is a group of three doublets ^{2}F, ^{2}P and ^{2}D. If it is assumed that the primary ion is in its ground state as above, available molecular terms reduce to the doublets $^{2}\Pi$ and $^{2}\Sigma^{-}$. Then the donor channels from the $^{2}\Pi$ are divided among three paths terminating to the ^{2}F, ^{2}P and ^{2}D terms. The other ones from the $^{2}\Sigma^{-}$ correlates only to the ^{2}D term. As a result, the ^{2}D terms should be most populated. This prediction, however, disagrees with the estimation from excitation cross-sections, as seen in Fig. 4(a).

Ions extracted from a plasma ion-source are usually contaminated by metastable ions. If all the primary ions are the ground-state ions, the formation process of the ArII 4p'-state should be a two-electron process; an electron capture $Ar^{2+} + e^{-}$ and an excitation $^{3}P \rightarrow {}^{1}D$. Such a process has in general a rather small cross-section compared with the one-electron process. Moreover, crossing distances become quite large ($R_c \simeq$ 20-30 a.u.); diabatic transitions do not seem to occur.

These facts naturally lead us to assume that the metastable ion $Ar^{2+}(3p^4, {}^1D)$ is responsible for formation of the 4p'-state. Then the formation process is a single-electron process and R_c is less than 10 a.u. Possible molecular terms arising from the reactant pair, $Ar^{2+}(3p^4, {}^1D) + Na(3s, {}^2S)$, are $^2\Sigma^+(2)$, $^2\Pi(4)$ and $^2\Delta(4)$, where each figure in parentheses represents the number of the respective *donor* channel. This procedure gives another population distribution different from that obtained just before, as seen in Fig. 4(b). The revised population distribution is in good agreement with the one estimated from excitation cross-sections. The present statistics reveals a metastable ion in the primary ion beam.

Similar statistical consideration can be applied to the process of electron capture into the ArII 4d-state; $Ar^{2+} + Na \rightarrow Ar^+(3p^4[{}^3P]4d) + Na^+({}^1S)$. Six terms such as ^4D, ^4F, ^4P, ^2F, ^2P and ^2D are predicted from the 4d-state. Emission lines from these terms are very weak and no emission can be detected from the ^2D and ^2P terms and from $^4D_{1/2}$, $^4F_{3/2}$, $^4P_{1/2}$ and $^4P_{3/2}$. Therefore, comparison between the statistical estimation and the experimental one is incomplete, and is made among the terms observed, as seen in Fig. 5. There is some discrepancy between them in particular for the ^2F and ^4P terms. This may be in part due to the large endothermicity of reactions for formation of the ^2F and ^4P terms and in part due to inaccuracy of measurements of weak radiation.

2d) Relative population distribution among multiplets

Here we examine the relative population among the fine-structure states, multiplets, of a given term. Figure 6 shows its estimation from excitation cross-sections at 8 keV together with the relative statistical weight of the multiplet $(2J+1)/(2J_{max}+1)$ for the ArII 4p-, 4p'- and 4d-states. Multiplets of high-J values are much populated for all the terms observed, and the relative population distribution among the multiplets is proportional to their statistical weight. In other words, it appears to be governed by statistics for the product pair only.

Such a feature is rather surprising. When a molecule is formed , a space quantization of the electronic angular momentum takes place along the internuclear axis. The resultant angular momentum including the spin Ω is atmost 5/2 for the molecular states resulting from the reactant pair, either $Ar^{2+}(^3P)$ + Na or $Ar^{2+}(^1D)$ + Na. Therefore, no channel should connect with the product multiplets of J>5/2. Actually, such multiplets as 4p $^4D_{7/2}$, 4p' $^2F_{7/2}$, 4d $^4F_{7/2,9/2}$ and 4d $^4D_{7/2}$ are most populated, as seen in Fig. 6. This fact strongly suggests that redistribution of the population among multiplets takes place during the collision time. Such a redistribution may be caused by another type of coupling, i.e., spin-orbit recoupling.[11] Separations in energy among the multiplets are smaller than those among the terms. On the basis of the uncertainty principle, it is expected that the interaction region of spin-orbit recoupling is larger than that of radial coupling at several-keV collisions; the recoupling may be effective in the separated-atomic region rather than in the molecular region.

§3. Energy Dependence of Excitation Cross-Sections

We examined the energy dependence of emission cross-sections for three emission lines, each of which was from the term of different electron-configuration states, 4p ^{4}S, 4p' ^{2}D and 4d ^{2}F (see Fig. 3 in I). No cascading transitions to the 4p'- and 4d-states was observed; the cascading effect on the 4p ^{4}S term was estimated to be smaller than 3 %. Therefore, the corresponding excitation cross-sections can be easily obtained as a function of energy, and are shown in Figs. 7 (a), (b) and (c) by open circles.

The excitation cross-section based on the Landau-Zener (L-Z) formula can be calculated from the initial and final diabatic potential energy curves H_{11} and H_{22}, and from the coupling matrix element H_{12} at the psuedocrossing R_c. If the relative kinetic energy is much greater than the potential enrgy H_{11}, the cross-section for the present collision system, $Ar^{2+} + Na \rightarrow Ar^{+*} + Na^+ + \Delta E$, can be expressed in the following form,[2,12]

$$Q = 4\pi R_c^2 \, I(\eta) P_{12} \, , \tag{3.1}$$

where

$$I(\eta) = \int_1^\infty \exp(-\eta x)\{1 - \exp(-\eta x)\} x^{-3} dx, \tag{3.2}$$

and

$$\eta = \frac{2\pi}{v_0}\left(\frac{H_{12}}{\Delta E}\right)^2. \tag{3.3}$$

Here the polarization interaction is neglected, because we consider transitions at large internuclear separations. Then, $R_c = 1/(\Delta E)$. All the quantities are in atomic units. The quantity v_0 is the relative velocity at the infinite separation, and P_{12} the probability that the system approaches along the potential curve 1 and then separates along the curve 2.

According to Olson, Smith and Bauer[6], the coupling matrix element H_{12} can be estimated from the reduced coupling matrix element H_{12}^* and the reduced crossing distance R_c^* as follows:

$$H_{12}^* = 1.0\ R_c^*\ \exp(-0.86R_c^*) \qquad (3.4)$$

with

$$H_{12} = \sqrt{I_a I_b}\ H_{12}^* \quad \text{and} \quad R_c^* = \frac{\sqrt{I_a} + \sqrt{I_b}}{2} R_c \qquad (3.5)$$

where I_a and I_b are the binding energy of Ar^{+*} and Na. The Olson-Smith-Bauer (O-S-B) cross-section Q^{OSB} is given by substitution of the coupling matrix H_{12} obtained from the above equations into eqs. (3.1) to (3.3).

Since the L-Z theory is the two-state approximation, there still remains the problem of determination of P_{12} in the case of multiple crossings and states. Salop and Olson generalized the L-Z formula to such a case by summing over possible paths necessary to make a transition.[13] Their generalization is reasonable for the case of many but well-separated states. As discussed in the preceding section, molecular terms terminating to the same nl-state of ArII are considered to be quasi-degenerate, whereas the ones terminating to different nl-states are well separated. Therefore,

for the formation process of the j-th term of the ArII nl-state, we conveniently assume that P_{12} is expressed by the product: $P_{12} = P_t \times P_s$; P_t is the probability for formation of the specific j-th term in a given nl-state, and P_s for formation of the specific nl-state in competing processes to form different nl-states. Then, P_t is determined by the present statistics, so that P_t is independent of energy. As for P_s, we simply assume that $P_s = 1$ and then $P_{12} = P_t$†, because we are concerned mainly with the relative population distribution among the terms of a given nl-state.

---

†On the treatment of competing processes, this simple assumption is questionable. However, the energy region in which electron capture occurs predominantly may be quite different among those processes. Therefore, the assumption may be accepted for the process of a large cross-section among competing processes.

The energy dependence of Q^{OSB} is now compared with that of the excitation cross-section obtained experimentally Q_{exp} for the 4p ^{4}S term. The former is shown in Fig. 7(a) by a broken curve, where the peak value is normalized to the maximum value of Q_{exp}. The two cross-sections exhibit different energy dependence. The discrepancy may be due to inaccuracy of the O-S-B formula, as Olson et al. pointed out.[6] They indicate the 95% confidence level on both the pre-exponential factor and the exponential one by examining deviations of the data compiled. However, variations of the two factors even within this confidence level results in uncertainty in H_{12} with a factor of ten for the present case. The best-fit for the experimental curve is obtained with the H_{12}

value of 6.3×10^{-3} a.u. and is shown by a solid curve in Fig. 7(a), whereas the O-S-B formula gives the value of 3.0×10^{-3} a.u.

Similar discrepancy between Q^{OSB} and Q_{exp} is seen for the $4p'\ ^2D_{5/2}$ term. If the metastable ion $Ar^{2+}(^1D)$ is responsible for the production of the 4p'-state as mentioned in §2, the O-S-B formula gives the H_{12} value of 5.4×10^{-3} a.u. and the Q^{OSB} obtained is shown by a broken curve in Fig. 7(b), where the peak value of Q^{OSB} is normalized to the maximum value of Q_{exp}. Because Q_{exp} has no peak in this energy region, it is difficult to estimate the best-fit value of H_{12}, but it would be smaller than 5.4×10^{-3} a.u.

For the formation of the 4d-state, the measured cross-section seems to be independent of energy. Since the process is endothermic, the L-Z theory can not be applied to this process, and the formulation given by Demkov[3] and Olson[7] will be available. However, such an energy dependence will be difficult to understand theoretically. The formation process of the 4d-state has a small cross-section and competes with other processes having larger cross-sections such as the formation of the 4p-state, so that the energy dependence may be affected with these competing processes.

Let us return to the L-Z formulae (3.1) to (3.3). On our assumption, $P_{12} = P_t$, the energy dependence of excitation cross-sections is determined by $I(\eta)$ or η. If $H_{12}/(\Delta F)$ has the same value for all the terms arising from the same nl-state, the relative population distribution among the terms will be independent of energy and will be determined mainly with P_t, because R_c is nearly the same in those terms. Although the energy dependence was not examined in detail for individual excitations, the relative population distribution among the terms at 4 keV is nearly the same as

the one at 8 keV for the 4p'-state. On the other hand, there is some difference between those distributions at 4 keV and 8 keV for the 4p-state. This may be due to the difference in $H_{12}/(\Delta E)$ among the terms, because H_{12} is quite sensitive to the value of R_c (see eq. (3.4)), and because the R_c values corresponding to individual terms in the 4p-state are distributed over the region wider than in the 4p'-state.

Assume that $H_{12}^* = 0.645 \exp(-0.7R_c^*)$, which leads to the best-fit value of H_{12} ($=6.3\times10^{-3}$ a.u.) for the ^4S term. Then Q^{OSB} can be evaluated at 4 and 8 keV for each term, provided that P_t follows from statistics for the terms of the 4p-state. The excitation cross-sections obtained in such a way are in agreement with the experimental ones within a factor of two for all the terms and at both the energies. The relative population distribution calculated is compared with the experimental one in Fig. 8. The two distributions change quite similarly, when the ionic energy changes from 4 to 8 keV. Therefore, it is concluded that the relative population distribution among the terms of the same electron-configuration state is determined mainly with statistics and slightly modified owing to their different energy dependence at several-keV collisions.

§4. Concluding Remarks

We have seen that two types of coupling are responsible for electron-capture into the ArII nl-state by Ar^{2+} impacts on Na at several-keV collisions. The relative population distribution among the product atomic terms is well explained in terms of

statistics based on the building-up principle of molecule under the radial coupling scheme. The relative population distribution among the multiplets within a given term is proportional to their statistical weight; spin-orbit recoupling is responsible for the population mechanism.

The validity of the present statistics depends on the degree of mixing of adjacent molecular states during the collision, but it will be applicable widely to the collision process involving multiply-charged-ions, because dominant inelastic collisions take place mostly under the radial coupling scheme. The present statistical model will be an useful means in treatment of such processes, because it predicts the population distribution among the product terms and among the multiplets in a very simple procedure.

Acknowledgments

This work was supported in part by the Grant-in-Aid for Special Project Research No. 111011 from the Ministry of Education and was done under the Collaborating Research Program at Institute of Plasma Physics, Nagoya University.

References

1) A.Matsumoto, S.Tsurubuchi, T.Iwai, S.Ohtani, K.Okuno and Y.Kaneko: J. Phys. Soc. Japan (to be submitted).

2) C.Zener: Proc. Roy. Soc. A137 (1932) 696.

3) Yu.N.Demkov: Soviet Physics-JETP 18 (1964) 138.

4) D.R.Bates: Proc. Roy. Soc. A257 (1960) 22.

5) D.R.Bates, H.C.Johnston and I.Stewart: Proc. Phys. Soc. 84 (1964) 517.

6) R.E.Olson, F.T.Smith and E.Bauer: Appl. Optics 10 (1971) 1848.

7) R.E.Olson: Phys. Rev. A6 (1972) 1822.

8) W.Lichten: Phys. Rev. 131 (1963) 229.

9) G. Herzberg: Molecular Spectra and Molecular Structure I.Spectra of Diatomic Molecules (D. van Nostrand,1950) 2nd ed., Chap. 6.

10) A.Russek: Phys. Rev. A4 (1971) 1918.

11) N.H.Tolk, J.C.Tully, C.W.White, J.Kraus, A.A.Monge, D.L.Simms, H.F.Robbins, S.H.Neff and W.Lichten: Phys. Rev. A13 (1976) 969.

12) D.R.Bates and B.L.Moiseiwitsch: Proc. Phys. Soc. A67 (1954) 805.

13) A.Salop and R.E.Olson; Phys. Rev. A13 (1976) 1312.

Table 1. Excitation cross-section Q_j for $Ar^{2+}(3p^4,{}^3P) + Na(3s,{}^2S) \rightarrow Ar^+(3p^4nl;j) + Na^+(2p^6,{}^1S)$ in $10^{-16}cm^2$, and relative population distribution among the terms of $Ar^+(3p^4nl;j)$ in %; a. experimental, b. statistics based on the building-up principle.

Term	Q_j	a.	Q_j	a.	b.
	4 keV		3 keV		
$3p^4({}^3P)4p$	31.05	100	58.84	100	100
${}^4P$	4.10	13	8.97	15	22.2
${}^4D$	9.30	30	21.18	36	33.3
${}^2D$	4.51	15	10.08	17	16.7
${}^2P$	4.09	13	8.25	14	11.1
${}^4S$	7.53	24	7.16	12	11.1
${}^2S$	1.53	5	3.21	6	5.6
$3p^4({}^1D)4p'$	14.73	100	19.92	100	100
${}^2F$	8.43	57	10.82	54	22.2, 43.3*
${}^2P$	2.10	14	3.49	18	55.6, 23.3*
${}^2D$	4.20	29	5.61	28	22.2, 33.3*
$3p^4({}^3P)4d$	3.72	100	4.04	100	100
${}^4D$	0.86	23	0.86	21	22
${}^4F$	1.24	33	1.38	34	36
${}^2F$	1.38	37	1.51	37	21
${}^4P$	0.24	7	0.30	7	21
${}^2P$	-	-	-	-	-
${}^2D$	-	-	-	-	-

*; statistics for $Ar^{2+}(3p^4,{}^1D) + Na \rightarrow Ar^+ + Na^+$.

Figure Captions

Fig. 1. Approximate diabatic potential curves for $Ar^{2+}(3p^4, {}^3P \text{ or } {}^1D) + Na(3s) \rightarrow Ar^+(3p^4nl) + Na^+(2p^6)$. Potential curve for the product pair, $Ar^+(3p^4nl) + Na$, is denoted by nl.

Fig. 2. Correlation between the reactant pair, $Ar^{2+}(3p^4, {}^3P) + Na(3s, {}^2S)$, and the product pair, $Ar^+(3p^4[{}^3P]4p) + Na^+(2p^6, {}^1S)$. $(Ar, Na)_i^{2+}$ denotes the molecular state arising from the reactant pair; $(Ar, Na)_f^{2+}$ from the product pair.

Fig. 3. Relative population distribution among the terms of $Ar^+(3p^4[{}^3P]4p)$. (I), experimental at 8 keV; (II), statistics based on the building-up principle of molecule.

Fig. 4. Relative population distribution among the terms of $Ar^+(3p^4[{}^1D]4p')$. (I), experimental at 8 keV; (II), statistics; (a), for $Ar^{2+}(3p^4, {}^3P) + Na \rightarrow Ar^+(4p') + Na^+$; (b), for $Ar^{2+}(3p^4, {}^1D) + Na \rightarrow Ar^+(4p') + Na^+$.

Fig. 5. Relative population distribution among the terms of $Ar^+(3p^4[{}^3P]4d)$. (I), experimental at 8 keV; (II), statistics.

Fig. 6. Relative population distribution among the fine-structure states normalized at the J_{max} state. Soild lines, experimental; broken lines, statistical weight $(2J + 1)$. (a), $Ar^+(3p^4[{}^3P]4p)$; (b), $Ar^+(3p^4[{}^1D]4p')$; (c), $Ar^+(3p^4[{}^3P]4d)$.

Fig. 7. Energy dependence of excitation cross-sections.
(a) for ArII ($3p^4[^3P]4p$, $^4S_{3/2}$); open circles, Q_{exp}; broken curve, Q^{OSB} from $H_{12} = 3.0 \times 10^{-3}$ a.u.; solid curve, Q^{OSB} from $H_{12} = 6.3 \times 10^{-3}$ a.u.
(b) for ArII ($3p^4[^1D]4p'$, $^2D_{5/2}$); open circles, Q_{exp}; broken curve, Q^{OSB} from $H_{12} = 5.4 \times 10^{-3}$ a.u.
(c) for ArII ($3p^4[^3P]4d$, $^2F_{7/2}$); open circles, Q_{exp}.

Fig. 8. Relative population distribution among the terms of ArII ($3p^4[^3P]4p$). Left pair of bars on each term at 4 keV; right pair at 8 keV. (I), experimental; (II), theoretical.

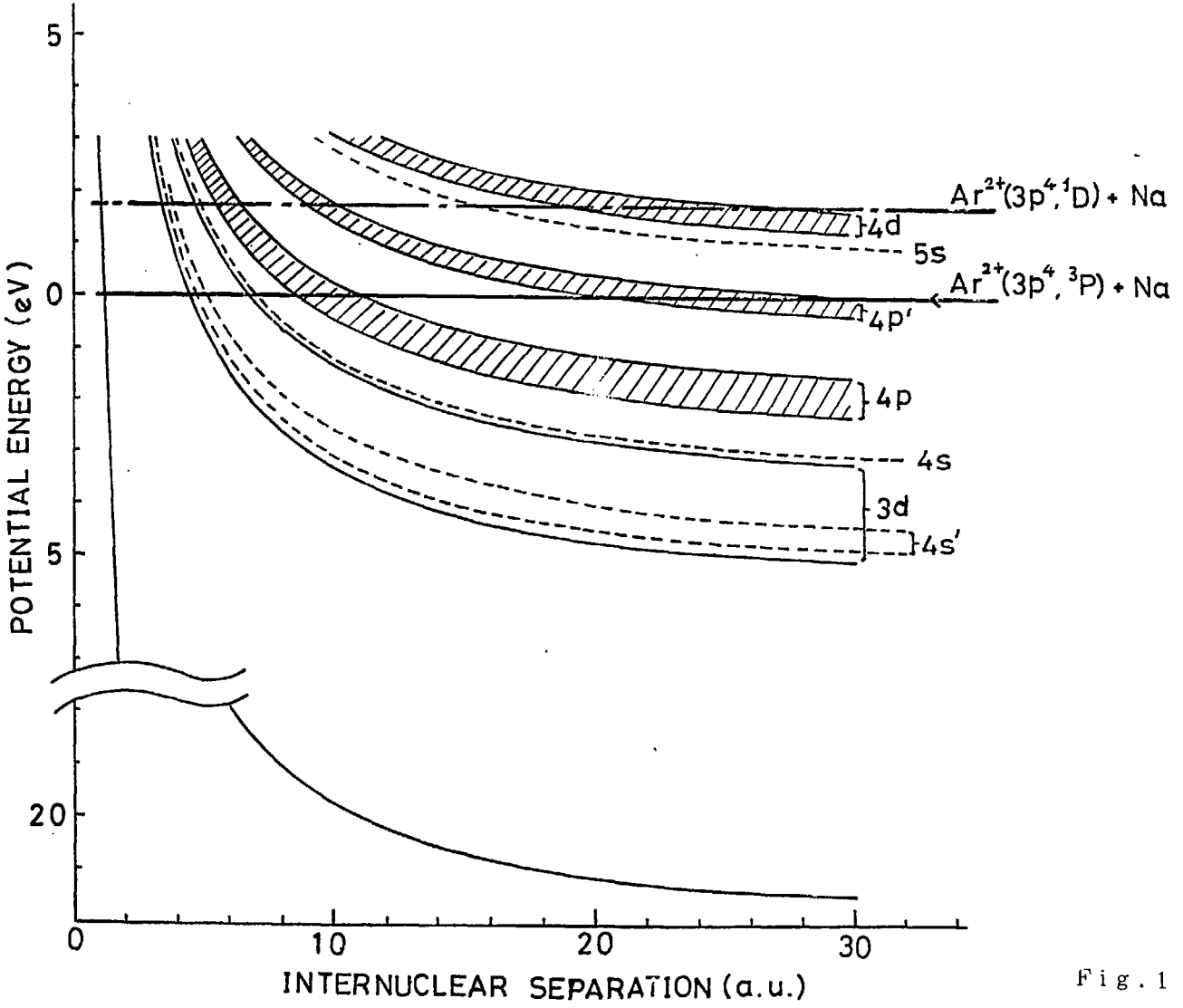
5
0
5
20
POTENTIAL ENERGY (eV)
0
10
20
30
INTERNUCLEAR SEPARATION (a.u.)
Ar2+(3p4, 1D) + Na
Ar2+(3p4, 3P) + Na
4d
5s
4p'
4p
4s
3d
4s'

Fig. 1

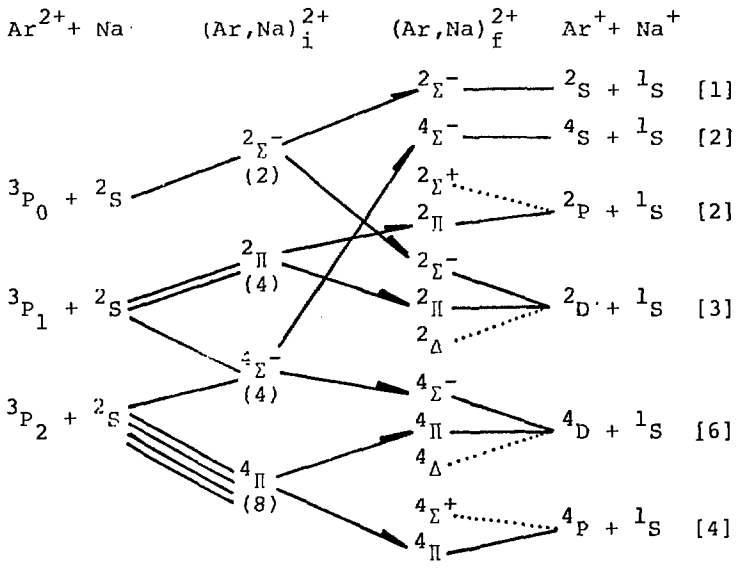
Ar2+ + Na
(Ar,Na)i2+
(Ar,Na)f2+
Ar+ + Na+
3P0 + 2S
3P1 + 2S
3P2 + 2S
2Σ− (2)
2Π (4)
4Σ− (4)
4Π (8)
2Σ−
4Σ−
2Σ+
2Π
2Σ−
2Π
2Δ
4Σ−
4Π
4Δ
4Σ+
4Π
2S + 1S [1]
4S + 1S [2]
2P + 1S [2]
2D + 1S [3]
4D + 1S [6]
4P + 1S [4]

Fig. 2

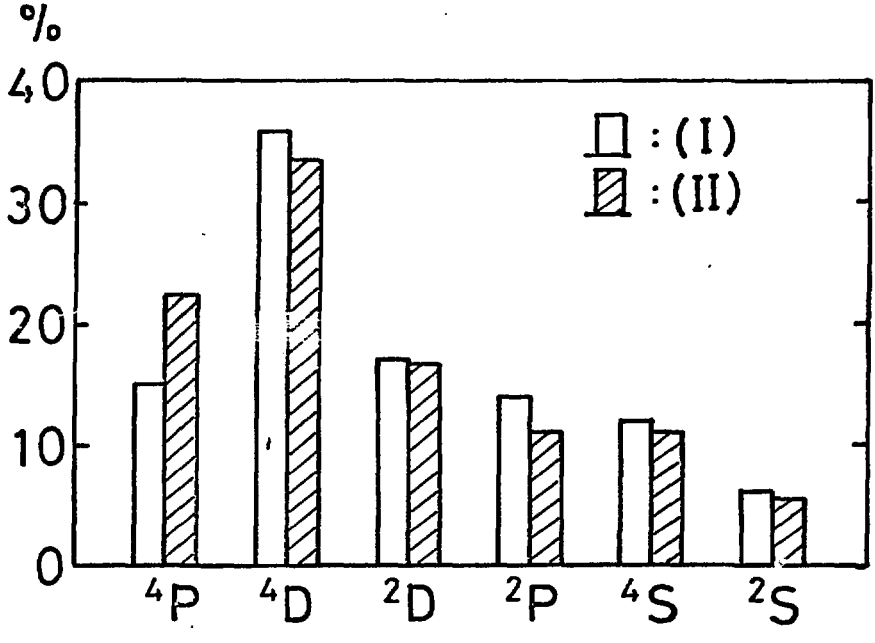

Fig. 3

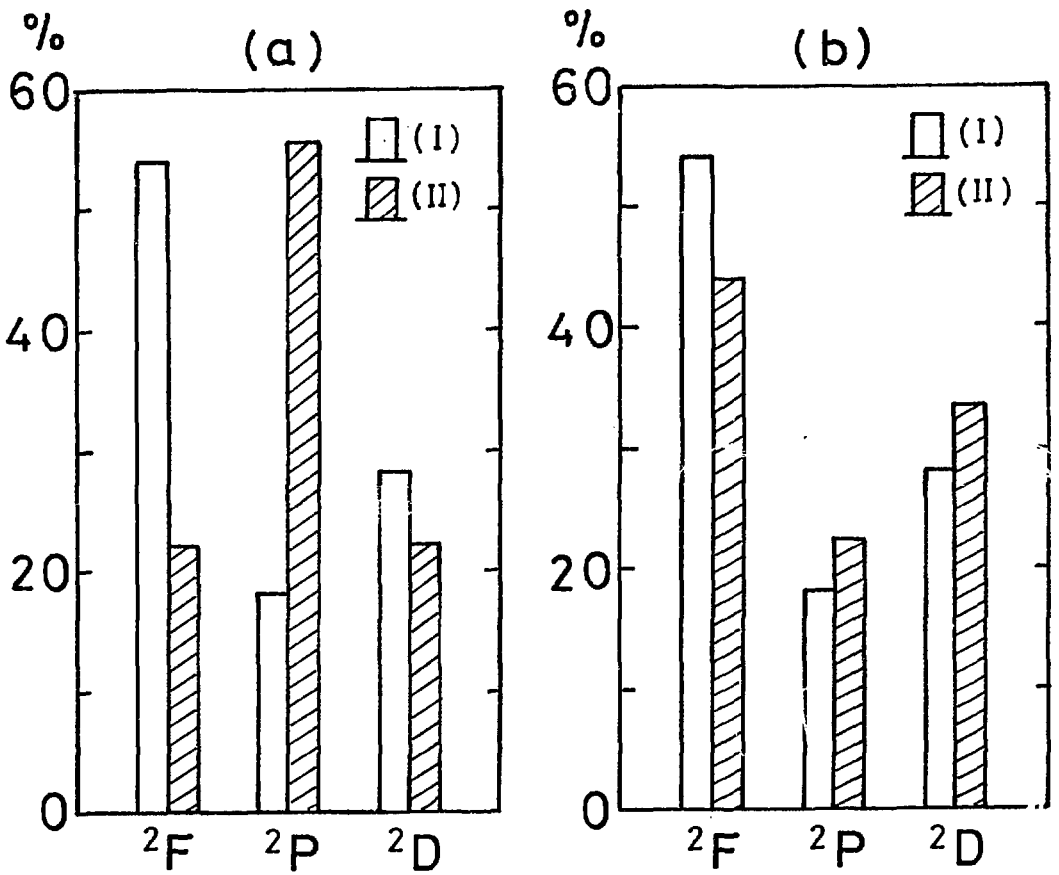

Fig. 4

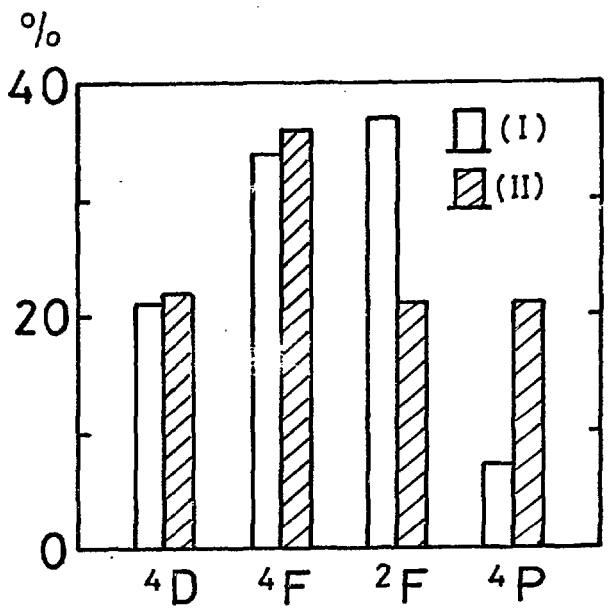

Fig. 5

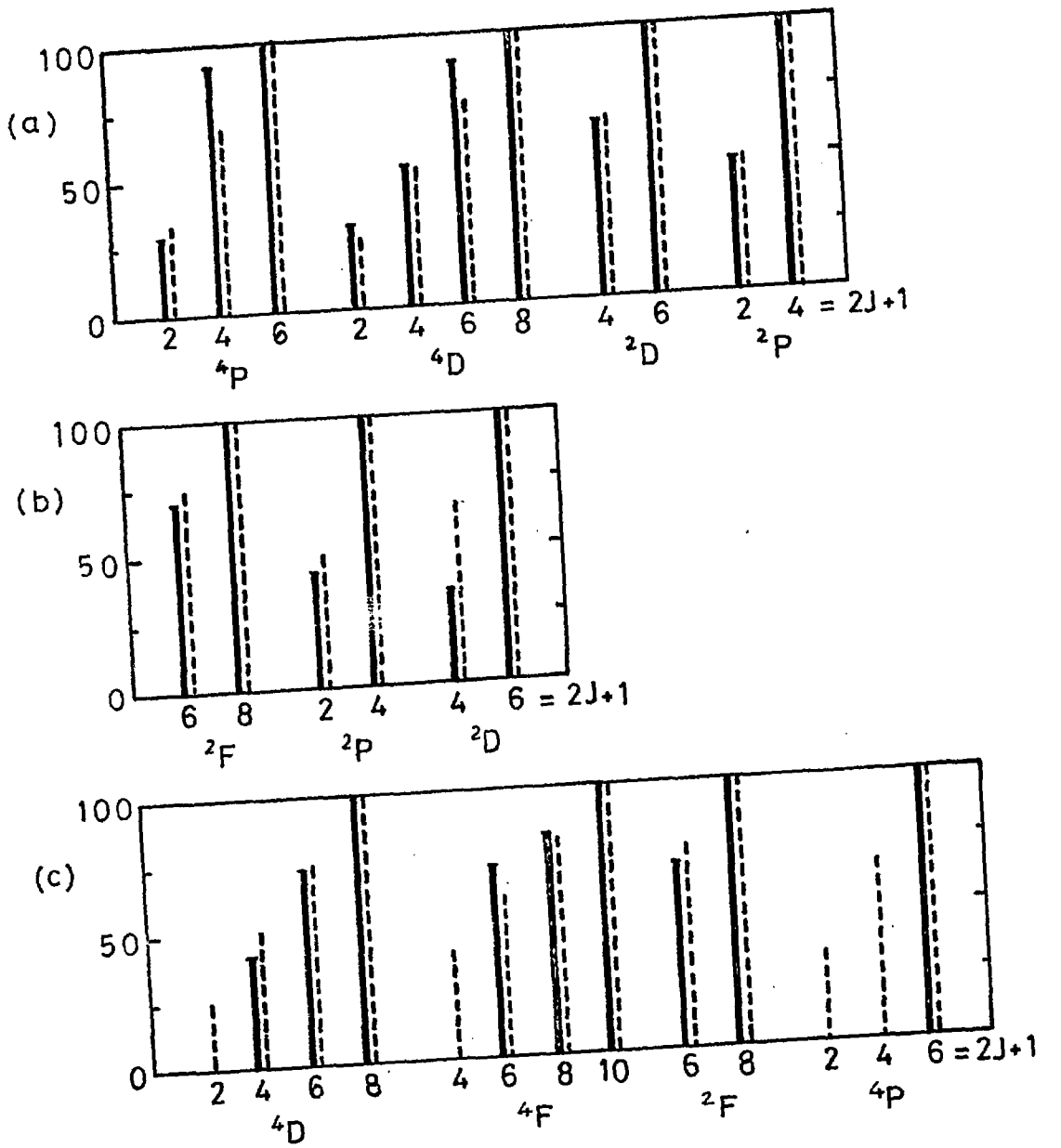
(a)
100
50
0
2 4 6 2 4 6 8 4 6 2 4 = 2J+1
4P 4D 2D 2P
(b)
100
50
0
6 8 2 4 4 6 = 2J+1
2F 2P 2D
(c)
100
50
0
2 4 6 8 4 6 8 10 6 8 2 4 6 = 2J+1
4D 4F 2F 4P

Fig. 6

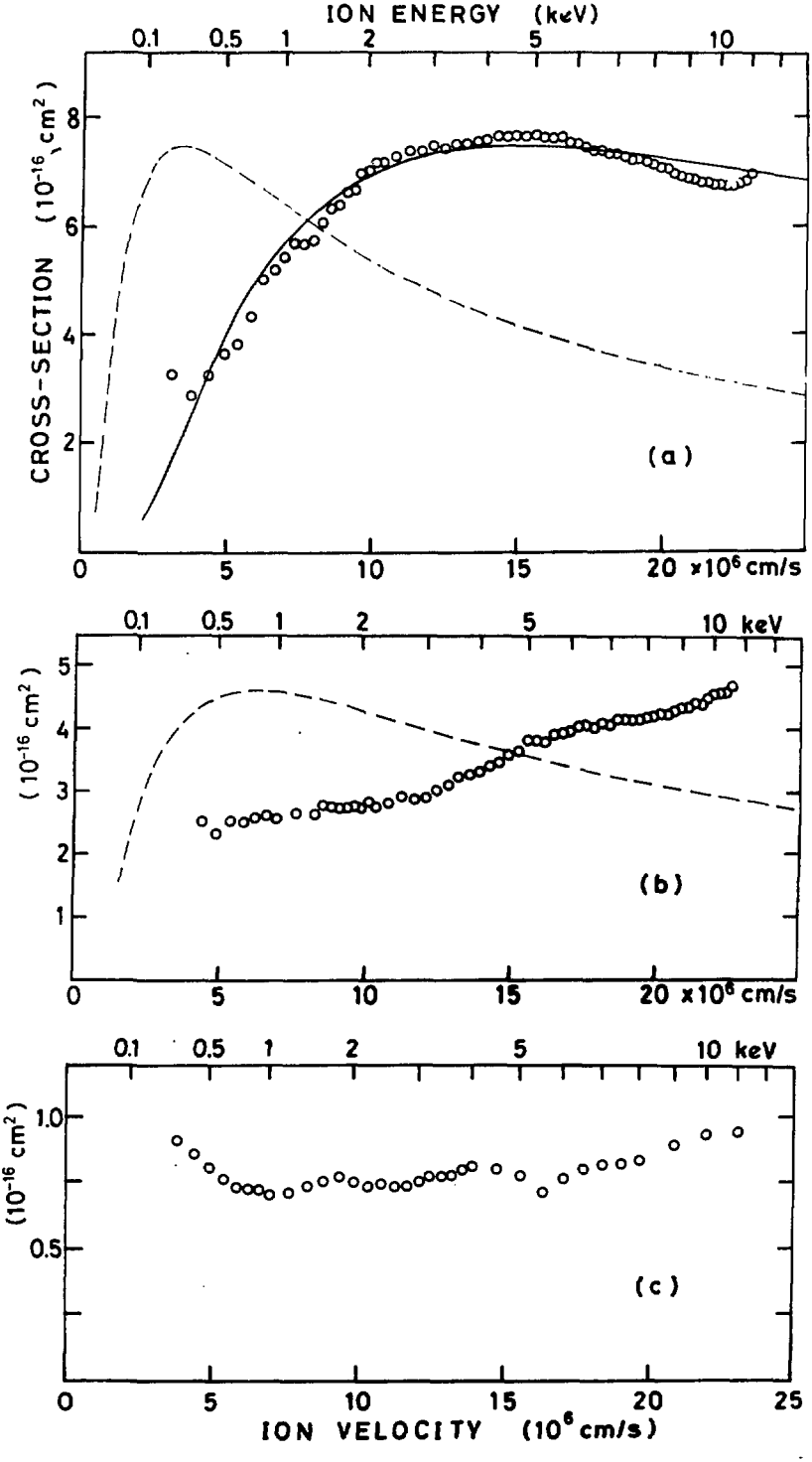
ION ENERGY (keV)
0.1
0.5
1
2
5
10
CROSS-SECTION (10^{-16} cm^2)
8
6
4
2
(a)
0
5
10
15
20 x10^6 cm/s
0.1
0.5
1
2
5
10 keV
(10^{-16} cm^2)
5
4
3
2
1
(b)
0
5
10
15
20 x10^6 cm/s
0.1
0.5
1
2
5
10 keV
(10^{-16} cm^2)
1.0
0.5
(c)
0
5
10
15
20
25
ION VELOCITY (10^6 cm/s)

Fig. 7

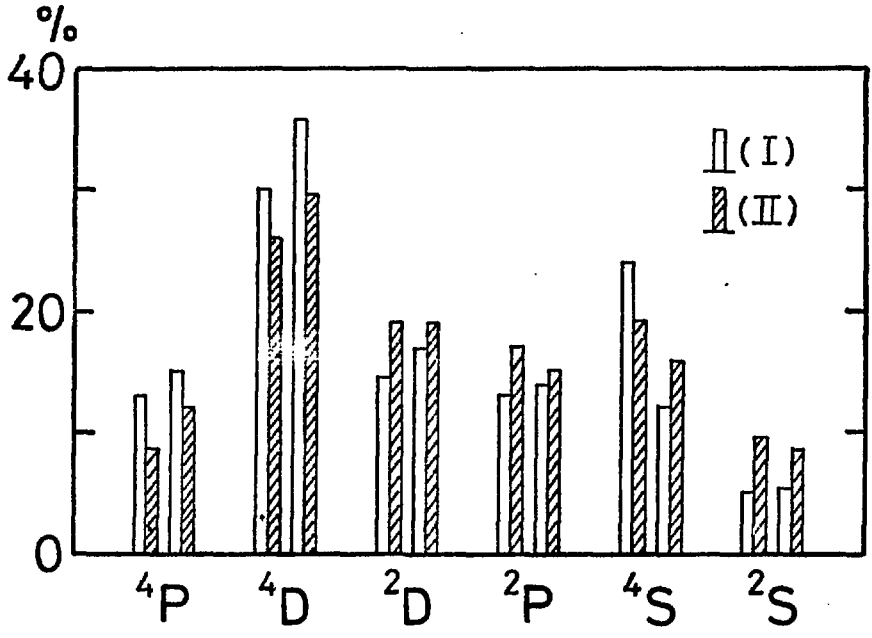

Fig. 8